Intentional Controlled Islanding and Risk Assessment: A Unified Framework

J. Quirós-Tortós, *Senior Member, IEEE*, P. Demetriou, *Student Member, IEEE*,
M. Panteli, *Member, IEEE*, E. Kyriakides, *Senior Member, IEEE*, and V. Terzija, *Fellow, IEEE*

***Abstract*--Power systems are prone to cascading outages leading to large-area blackouts, and intentional controlled islanding (ICI) can mitigate these catastrophic events by splitting the system into sustainable islands. ICI schemes are used as the last resort to prevent cascading events; thus, it is critical to evaluate the corresponding system risks to ensure their correct operation. This paper proposes a unified framework to assess the risk of ICI schemes. First, a novel ICI method to create islands with minimum power imbalance is presented. Further, a risk assessment methodology is used to assess the probability and impact of the main operational modes of the ICI scheme. The unified framework provides insights on the benefits of implementing ICI, considering the uncertainties related to its reliability. The ICI scheme is demonstrated using the IEEE 9-bus system. The proposed unified framework is then fully deployed on the actual power system of Cyprus. Multiple case studies on the real network are created to demonstrate the adaptability and robustness of the proposed scheme to different system conditions. The adoption of the unified framework highlights that the system risk significantly reduces with the ICI in service, even when the reliability uncertainties associated with the scheme are considered.**

***Index Terms*—Blackout prevention, intentional controlled islanding, system splitting, reliability assessment, risk assessment.**

I. Introduction

POWER systems are prone to cascading outages leading to large-area blackouts, and intentional controlled islanding (ICI) is an effective, corrective control action to mitigate these catastrophic events [1]–[3]. ICI is aimed to be used as the last resort to prevent blackouts; usually after severe contingencies, but before the system becomes uncontrollable and start losing its integrity. It determines in real-time (within few seconds in practice [1]) a set of lines to be disconnected across system to create sustainable and stable islands [4]–[13].

Several ICI methods are reported in the literature [4]–[13]. The slow coherency theory is effectively used in [4]–[6] to split the system across weak connections; however, this approach might not account for changes in the topology of the network, which can have an effect in the coherency results. Spectral clustering-based ICI methods are presented in [7]–[9]. However, the unsupervised nature of these approaches makes difficult the introduction of ICI constraints (e.g., generator coherency, load-generation balance) in the problem. Ordered binary decision diagrams (OBDD) are also used [10]–[12]. Although OBDD-based ICI methods can search for a solution across the whole search space, the size of the network to be partitioned needs to be reduced to less than 40 nodes to obtain solutions within realistic time frames (i.e., seconds) [9].

Although the existing approaches can find an islanding solution, the potential sources of misoperation of the ICI schemes and the impact of the undesirable events on the system reliability have not yet been assessed, as it has been done for others [14]–[17]. These types of studies can conduct highly accurate reliability modeling of wide-area protection schemes, both at a component and at a scheme level. This is particularly important as the misoperation of wide-area protection schemes can have a significant impact on the network reliability. Thus, a reliable and timely implementation of ICI schemes, and in general the System Integrity Protection Schemes (SIPS), is critical for boosting the reliability of electrical power systems.

ICI schemes are highly complex, composed of several components for field data acquisition, triggering event detection and implementation of the islanding solution. This might lead to severe reliability issues, i.e., inability of the ICI scheme to operate as initially designed, due to the numerous sources of possible malfunctions in the ICI components. Similar to other SIPS, the main failure modes of ICI schemes are (i) the failure to operate when needed and (ii) the incorrect (i.e., spurious) operation when there is no disturbance in the system. The impact of these failure modes varies and depends on the evolving system conditions. An example that shows the impact of such schemes' misoperation is the Irish disturbance of August 2005 [18]. Due to false communication signaling, the system was incorrectly split into two areas, resulting in the loss of 326,000 customers in the Republic of Ireland and 74,000 customers in Northern Ireland. It is, thus, critical to develop and apply risk assessment techniques to estimate and mitigate the risk introduced to the network by such events.

This paper proposes a unified framework to assess the risk of ICI schemes on the electrical power system. First, a novel ICI scheme based on graph theory is developed to determine an islanding solution that creates islands with minimum power imbalance, while ensuring that each island contains only coherent generators. The proposed ICI scheme, designed here for the case when only two electrical islands are needed, enables the exclusion of critical branches (e.g., transformers) and explores the vast combinatorial space to find the optimal solution. The new ICI scheme is tested using the dynamic model of the IEEE 9-bus and a full model of the Cypriot network. Time-domain simulations are used to demonstrate its effect-

This work has been partly funded by the University of Costa Rica and the European Commission 7th Framework Program under grant FP7-ERC Advanced Grant -291508. J. Quirós-Tortós is with the EPERLab of the School of Electrical Engineering, University of Costa Rica, Costa Rica. P. Demetriou and E. Kyriakides are with the KIOS Research Center for Intelligent Systems and Networks, Department of Electrical and Computer Engineering, University of Cyprus, Cyprus. M. Panteli and V. Terzija are with the School of Electrical and Electronic Engineering, The University of Manchester, UK. (e-mails: jairoquirostortos@ieee.org, demetriou.k.panayiotis@ucy.ac.cy, mathaios.panteli@manchester.ac.uk, elias@ucy.ac.cy, terzija@ieee.org).

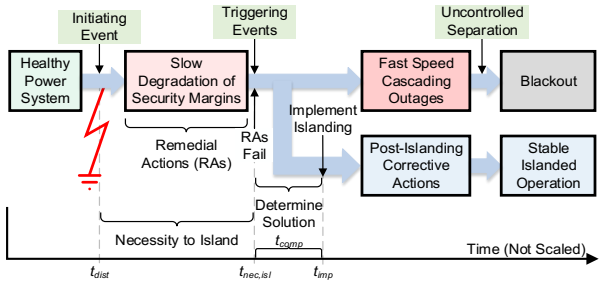

Fig. 1. General framework of the intentional controlled islanding [9]

tiveness. Multiple scenarios in the real system are developed to demonstrate its adaptability to different realistic conditions.

Crucially, further to the new ICI scheme, this paper proposes a risk assessment methodology for estimating the risk introduced by the ICI failure modes. The ICI and the risk assessment proposals result in a unified framework that provides insights on the benefits and risks of implementing ICI schemes in the power systems, considering different sources of uncertainties and concerns related to their reliability. This unified framework is applied on the ICI scheme of the Cypriot system, which gives an indication of the network risk to large-area blackouts with the proposed ICI scheme armed, or disarmed. The simulation results show that having the ICI scheme in operation reduces the overall system risk, providing useful suggestions on the network reliability enhancement and investment strategies. Further studies, e.g., adding redundancy and varying the test interval of the proposed ICI scheme, provide valuable insights on the aspects affecting its reliability.

II. Intentional Controlled Islanding

This section presents the ICI method that is based on the graph theoretic cut-set matrix [19], [20]. For simplicity, the case in which a system must be split into two islands is detailed. A recursive bisection approach (partitioning into two), as those in [10], [12], can be adopted to create more islands.

A. The Concept of ICI

Fig. 1 illustrates the general concept of ICI [9], which is associated with the blackout progress [21]. Blackouts might be caused by the uncontrolled separation of the system [1], [2]. This can be initiated by a single event that results in the slow degradation of the grid and the reduction of the security margins. Remedial actions (RAs) are typically applied to avoid this degradation; however, RAs can fail or not be implemented on time. Indeed, operators might not be aware of the situation [22]. These factors can cause the system to enter the fast speed cascading outages, triggering the uncontrolled disconnection of components and resulting in large-area blackouts.

To mitigate cascading outages leading to blackouts, ICI can be used [1], [2]. When the vulnerability analysis identifies the necessity to split the system, an ICI method can be used to find the optimal islanding solution. The time of defining the necessity to island the system typically depends on the vulnerability analysis [9] and is denoted in Fig. 1 by $t_{nec,isl}$.

An ICI method should then find, in an adaptive manner, an optimal islanding solution. To avoid any delay, the ICI method must be efficient to reduce the computational time, denoted by t_{comp}. When the solution is determined, it would be implemented at time t_{imp}. Then, due to the inherent characteristics of the system, additional corrective measures (e.g., fast valving and load shedding) may be needed to ensure that each island retains its security margins in the post-islanding phase [4]–[13]. Each island is then expected to reach a stable operation, and after a certain period, the whole system should be restored to the pre-disturbance healthy system by synchronizing the islands and connecting them into an integrated system.

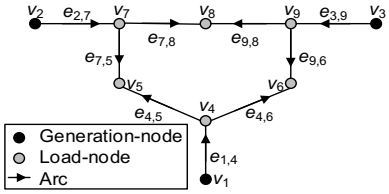

Fig. 2. Graph representation of IEEE 9-bus test system

B. Graph Theory Background

A power system with n buses and m generators can be represented as a weighted and directed graph $G = (V, E, \omega)$. The elements $v_i \in V$, $i = 1,\ldots,n$, and $e_{ij} \in E \subset V \times V$, $i, j = 1,\ldots,n$, denote the nodes (buses) and arcs (branches, from node i to node j) of G, respectively. The power flow is used to define the direction of the arc. The number $w_{ij} = \omega(e_{ij})$, $i, j = 1,\ldots,n$, represents the weight factor associated with the arc $e_{ij} \in E$. To accommodate network losses, w_{ij} is calculated as follows:

$$w_{ij} = \begin{cases} \dfrac{|P_{ij}| + |P_{ji}|}{2} & \text{if } e_{ij} \in E; \\ 0 & \text{otherwise.} \end{cases} \quad (1)$$

where P_{ij} and P_{ji} represent the active power flow in the branch from bus i to j, and from j to i, respectively. As an example, Fig. 2 shows a graph representation of the IEEE 9-bus test system used in this section to illustrate the ICI method.

To represent the m generation-buses of the system (black dots in Fig. 2), the subset $V_{GN} \subset V$ of generation-nodes, with elements $v_i^{GN} \in V_{GN}$, is defined. Therefore, the subset $V_{LD} = V \setminus V_{GN}$ of load-nodes (where \ denotes the set-theoretic difference and defines V_{LD} as the set of nodes in V that do not appear in V_{GN}), with elements $v_i^{LD} \in V_{LD}$, is defined to represent the $n - m$ load-buses (grey dots in Fig. 2).

1) Oriented Incidence Matrix

The oriented incidence matrix $\mathbf{M}$ of G represents the incidence among nodes and arcs, and is defined as follows [20]:

$$\mathbf{M} := [m_{ik}] = \begin{cases} 1 & \text{if arc } e_k = e_{ij} \text{ is incident from node } v_i; \\ -1 & \text{if arc } e_k = e_{ij} \text{ is incident to node } v_i; \\ 0 & \text{otherwise.} \end{cases} \quad (2)$$

2) Oriented Cut-set, Oriented Cut and Label of the Nodes

An oriented cut-set $E_S \subset E$ is the set of arcs to be removed to split G into r subgraphs $G_1,\ldots,G_r$, with node sets $V_1,\ldots,V_r$. For the case of two islands (more islands can be obtained applying recursive bisection [19], [20]), the oriented *cut* associated with E_S from V_1 to V_2 can be calculated as follows:

$$cut(V_1, V_2) = \left| \sum_{v_i \in V_1, v_j \in V_2} w_{ij} - \sum_{v_i \in V_2, v_j \in V_1} w_{ij} \right|. \quad (3)$$

Given the cut-set E_S, the label of a node defines the island that the node belongs to. For instance, if Fig. 2 is split across the cut-set $E_S = \{e_{7,5}, e_{4,6}\}$ the label of the nodes $\{v_1, v_4, v_5\}$ is "1" and the label of the nodes $\{v_2, v_3, v_6, v_7, v_8, v_9\}$ is "2".

In the ICI problem for minimal power imbalance, E_S consists of the arcs that represent the branches in the system to be disconnected to create the islands and the value of the cut corresponds to the power imbalance in the resulting island.

C. ICI Method for Minimal Power Imbalance

The ICI method proposed in this paper seeks to minimize the power imbalance (generation minus load) within each island, while ensuring that each one contains only coherent generators and that the islanding solution excludes critical branches. To create two islands, the coherent groups of generators can be denoted by V_{GN1} and V_{GN2}. When determining a solution, each of these dynamic groups of generators must be separated into different islands to help the transient stability of the system. In addition, the proposed method enables operators to exclude any branch from the solution, particularly those that are deemed to be unfeasible for islanding, e.g., transformers or critical lines. For this, the subset $E_C \in E$, which represents the branches that must not be disconnected, is defined.

The problem of minimizing the power imbalance within each island can then be formulated considering the power transfer between islands (i.e., V_1, V_2). Thus, the ICI problem for minimal imbalance to be solved here is defined as follows:

$$\min_{V_1,V_2}\left(\left|\sum_{v_i\in V_1, v_j\in V_2} w_{ij} - \sum_{v_j\in V_1, v_i\in V_2} w_{ji}\right|\right) \tag{4}$$

subject to

$$V_{GNk} \subset V_k, \text{ and } E_C \cap E_S = \varnothing.$$

The condition $V_{GNk} \subset V_k$ constrains every island (denoted by the subset V_k) to contain only coherent generators (denoted by the subset V_{GNk}). The second condition $E_C \cap E_S = \varnothing$ means that the ICI method only considers partitions with cut-sets E_S not containing any excluded-arc from E_C.

1) Methodology to Solve the ICI Problem

To solve the islanding problem formulated above (for two islands), the next steps are sequentially followed:

Step 1: Create the matrix **M** associated with G using (2). For this purpose, the topology of the network at the moment of islanding (following the severe event) must be used.

Step 2: Define the label of the generation-nodes. Generators in the same coherent group must have the same label to preserve their integrity (coherency constraint). Define the load-nodes as free-nodes. A free-node can be grouped into any island. Since the aim of the proposed ICI method is to find an islanding solution, instead of identifying the generators within each coherent group, this work can adopt the approach presented in the existing literature, such as those described in [23], [24].

Step 3: Define the excluded arcs E_C (unfeasible branches). To constrain these branches to be excluded from the solution, define both ends of each excluded arc with the same label.

Step 4: Build the indicator matrix, **X**, that contains combinations of node labels that would partition G. The combinations in **X** label certain nodes to be in a given island and combine the free-node labels. This is a combinatorial problem that can be effectively solved by computing the permutations with repetitions of the free-node labels [25]. Each combination in **X** also includes the labels for the generation-nodes and any other constrained nodes so that each combination supplies a set of labels that defines the island each node will be clustered into.

Step 5: Compute the constrained cut-set matrix **C**, also known as the *cut-edge* incidence matrix, as follows [20]:

$$\mathbf{C} = \mathbf{X}^T\mathbf{M} \tag{5}$$

This matrix is used in graph theory to represent all the cut-sets in a graph [20]. The *ik*-entry of **C** is non-zero if the implementation of the i^{th} cut-set requires the arc $e_k = e_{ij}$ to be removed to partition G. Each cut-set included in **C** represents the arcs to be removed to separate the elements of G that have different labels in the corresponding combination in **X**. Use the concept of the rank of G to remove unfeasible cut-sets (i.e., solutions that are not satisfying the generator coherency constraint or solutions that split the system into an incorrect number of islands). It is important to mention that a detailed description of matrices **X** and **C** is provided in [20].

Step 6: Compute the vector **w**, which is a column vector with the j^{th} row equal to the arc weight (1). For this purpose, the power flow at the moment of islanding must be used.

Step 7: Determine the power imbalance within each island induced by each of the cut-sets included in **C** as follows:

$$cut(V_1, V_2) = \mathbf{C}\cdot\mathbf{w} \tag{6}$$

The islanding solution that results in the minimal power imbalance (i.e., the – local – optimal solution) is then found by finding the minimal entry of $cut(V_1, V_2)$, i.e., $min(cut(V_1, V_2))$.

D. Adoption of Wide Area Measurements

The proposed ICI method uses Wide Area Monitoring Systems (WAMS) to determine the optimal islanding solution. Given that real-time measurements (with a sampling rate between 30 to 60 samples per second) can be gathered using WAMS, the method obtains the line power flows, which, in turn, serve to create the incidence matrix (connectivity of the network) and to compute the weight of the corresponding arcs.

E. Simulation Examples

To illustrate the effectiveness of the ICI method, the complete, dynamic model of IEEE 9-bus test system, including Automatic Voltage Regulators (AVRs) and governors, is used [26]. All times quoted are based upon simulations performed on a PC with 2.33 GHz dual core CPU and 8 GB RAM.

Testing case description: The original base load was increased by 25%, while maintaining the same power factor. This stresses the system and increases the likelihood of instability following a disturbance. The increment was equally distributed among the generators. At time $t = 0.1$ s, a three phase to ground fault occurs near bus 7 at line 5–7, and it is cleared after local relays open the faulty line at 0.38 s (i.e., 0.28 s after the fault occurred). The swing trajectories obtained are shown in Fig. 3. Given that no control actions are undertaken, two groups of generators are obtained after the fault, i.e., {1} and {2, 3}. Fig. 3 highlights that this disturbance results in a blackout quickly after the fault is cleared.

To avoid this blackout, the proposed ICI method is used. The necessity to split the system is considered to be at 0.45 s (i.e., 0.07 s after the fault is cleared). As the scheme is adaptive and considers the actual topology and state of the system, the information (power flow and topology) at $t = 0.45$ s is used. To preserve the integrity of the coherent generators, v_1 is labeled '1' and v_2 and v_3 are labeled '2'. The load-buses 5, 6 and 8 are defined as free-nodes. The set of excluded arcs $E_C = \{e_{1,4}, e_{2,7}, e_{3,9}\}$ is defined as they represent transformers.

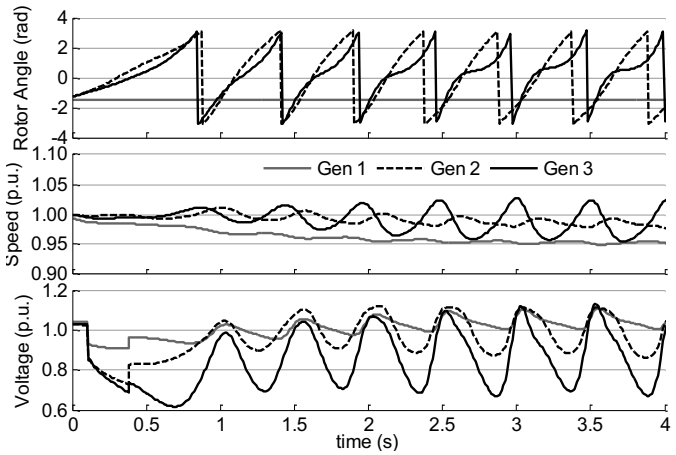

Fig. 3. IEEE 9-bus test system: Electrical behavior without islanding

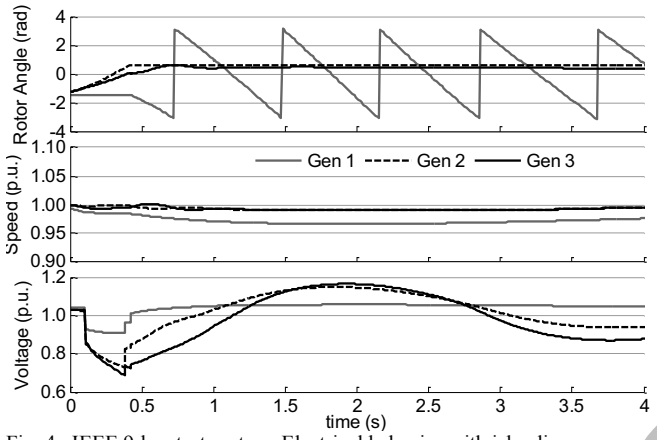

Fig. 4. IEEE 9-bus test system: Electrical behavior with islanding

The implementation of the ICI method identifies the optimal solution (for minimum imbalance) across lines 7-5 and 4-6. This solution was found in approximately 1.4 ms; islanding was undertaken at 0.4514 s. Fig. 4 shows the dynamic trajectories after implementing the optimal solution. Two coherent groups are created. Moreover, the frequencies of Island 1 and Island 2 are 0.976 p.u. and 0.995 p.u., respectively. Voltages also reach values close to the nominal. The results highlight that the splitting strategy successfully retains the frequency of the islands and the corresponding voltages within the thresholds; thus, preventing the blackout.

The ICI method can create more than two islands. To illustrate this, it is considered that three groups of generators are obtained after the fault: {1}, {2} and {3}. The method, in this case, will create two islands across lines 7-5 and 4-6 (like the case presented above), and will then split Island 2 into two more islands across line 9-8, for a total of three islands.

III. Risk Assessment Methodology

Fig. 5 shows the framework for assessing the risk introduced by the ICI failure modes. It must be clarified that this risk assessment procedure is performed offline and its purpose is to provide insights on the benefits and challenges when the risk implications related to the operational and failure modes of ICI schemes are taken into account. As it can be seen in Fig. 5, this procedure is composed of three steps: reliability assessment, impact assessment, and risk assessment. These steps are thoroughly presented and discuss below.

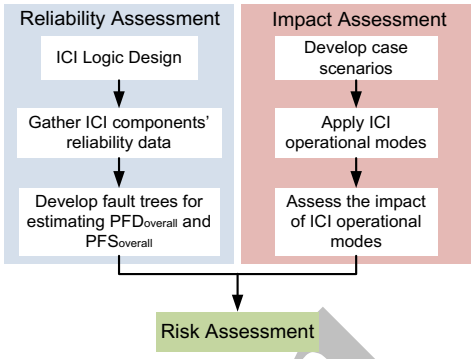

Fig. 5. Framework for assessing the risk of ICI failure modes

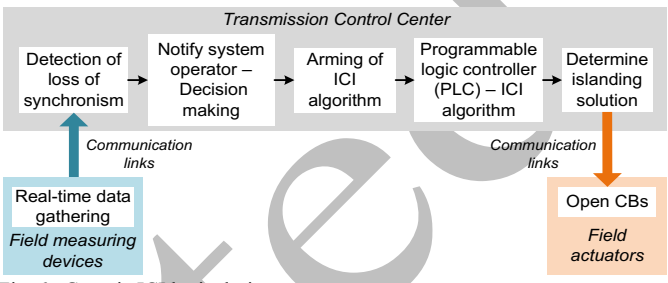

Fig. 6. Generic ICI logic design

A. Reliability assessment

As shown in Fig. 5, the main steps for assessing the reliability of an ICI scheme (real implementation) are the following:

Step 1: Develop the logic design of the ICI scheme. This would provide the components required for realizing the scheme. Fig. 6 shows a generic ICI logic design, where the key components of an ICI scheme can be seen, e.g., field measuring devices and actuators, communication links, and Programable Logic Controllers (PLCs). The main steps of the ICI scheme operation are the following (see Fig. 6):

i) Detection of loss of synchronism using real-time data.
ii) Alarm/notification to the Transmission System Operator (TSO) by the information/alarm processing system to manually arm in service the ICI method.
iii) Logic operation of ICI method (presented in section II) by the PLC to decide when and where to split the network.
iv) Automatic implementation/activation of the ICI scheme to send the inter-trip signals and open the appropriate circuit breakers (CBs) to split the network into stable islands.

Step 2: Gather the individual ICI components' reliability data. The main failure modes of ICI schemes considered here are (i) the failure to operate when needed and (ii) the spurious operation when the network is stable and no system splitting is required. Therefore, the components' reliability data required for assessing ICI reliability are the Mean Time To Failure (MTTF), and Mean Time To Fail Spurious (MTTFS).

Step 3: Estimate the probabilities of the ICI components' failure modes. These can be expressed using the probability of failure on demand (*PFD*) and probability to fail spurious (*PFS,* also known as probability to fail safe), respectively. Considering an exponential distribution for the failure rates of the components and that they are constant over their operating life, the ICI components' *PFD* and *PFS*, defined as the probability of failure to operate in a specified test interval (*TI*) and the probability of a spurious trip of the components in a given time period (*TP*) respectively, can be calculated as follows:

$$PFD = \lambda \frac{TI}{2} \quad \left(\lambda = \frac{1}{MTTF}\right) \tag{7}$$

$$PFS = \lambda_s \times TP \quad \left(\lambda_s = \frac{1}{MTTFS}\right) \tag{8}$$

where λ and λ_s are the failure and spurious rates of the components, and *TP* refers to the time period that λ_s is expressed (e.g., per week, month, year, etc.). It is considered that during the testing of the individual ICI components, the sources of failure to operate of the components are identified and removed, while a spurious operation is repaired once it occurs within the *TP* considered in the analysis.

Step 4: Estimate the probabilities of the ICI failure modes. To estimate the overall *PFD* ($PFD_{overall}$) and *PFS* ($PFS_{overall}$) of the scheme, fault tree analysis (FTA) is used [27]. FTA is a top-down deductive failure analysis that uses Boolean logic for determining the lower-level events or combination of events that lead to the occurrence of the top event. This technique has been effectively used for assessing the reliability of SIPS [15], [17]. The individual components' *PFD* and *PFS* calculated at Step 3 are inserted to the fault trees. Then, by using the logic operations of the fault trees, the $PFD_{overall}$ and $PFS_{overall}$ can be accurately estimated. These will be used for estimating the risk introduced to the system by the undesirable operations of the ICI scheme.

B. Impact assessment

The right side of Fig. 5 shows the main steps proposed in this paper for assessing the impact of ICI operational modes:

Step 1: Develop case scenarios for different operating conditions, for which the ICI would be needed. As the ICI scheme is to be used only during severe disturbances, these case scenarios should ideally reflect electrical events that typically result in a partial or complete blackout. Since the possible number of scenarios that could occur in a real power system is large, the focus of the development of these case scenarios will be on the "*worst-case scenarios*", similarly to the approach followed in previous works, such as [4]–[6].

Step 2: Apply the ICI operational modes to the case scenarios. Based on feedback from the TSO and worldwide practices [14], [28], three operational modes are considered here:

i) the failure of the scheme to operate when the loss of synchronism occurs;
ii) the incorrect operation of the ICI scheme before the system stability is compromised; and
iii) the success operation of the ICI scheme, as the ICI schemes' aim is not to eliminate the amount of customer interruptions but to mitigate it as much as possible. It would therefore result in an amount of load shedding for balancing the formed islands.

Step 3: Estimate the impact of ICI operational modes. The amount of load shedding (MW) is used in this work for this quantification as it is the main concern when blackout events take place. However, any other index can be used if desired.

C. Risk assessment

Following the reliability and impact assessment of the ICI operational modes (including both successful and failure modes), the risk with the ICI in operation is assessed, which is given by the product of the probability of the ICI operational mode and its impact. To determine if the ICI scheme benefits the reliability of the network, this risk is then compared to the risk of the electrical event without the ICI scheme.

The risk of the electrical event without the ICI scheme in operation is calculated as follows:

$$Risk = P(E) \times Im(E) \tag{9}$$

where *P(E)* and *Im(E)* are the probability of occurrence per year and impact of the electrical event (*E*), respectively.

To assign an economic value to the impact assessment, the Value of Lost Load (*VoLL*, €/MWh) is used. The impact is thus expressed as follows (measured in €/h):

$$Im(E) = L_{shed} \times VoLL \tag{10}$$

where L_{shed} is the amount of load shedding (MW) after (*E*).

The risk with the ICI scheme in operation is [28]:

$$Risk_{ICI} = Risk(Success) + Risk(Failure) + Risk(Spurious) \tag{11}$$

$$Risk(Success) = P(E) \times (1 - PFD_{overall}) \times Im(Success) \tag{12}$$

$$Risk(Failure) = P(E) \times PFD_{overall} \times Im(Failure) \tag{13}$$

$$Risk(Spurious) = P(\overline{E}) \times PFS_{overall} \times Im(Spurious) \tag{14}$$

The risk in (9) and (11)-(14) would thus be expressed in €/h. $PFD_{overall}$ and $PFS_{overall}$ are provided by the reliability assessment of the scheme and *Im(Success)*, *Im(Failure)* and *Im(Spurious)* are given by the impact assessment of the ICI operational modes (in terms of load shedding) for the different scenarios developed, which are quantified using (10). The risk of failure to operate is estimated upon the occurrence of the electrical event, and the risk of spurious operation is assessed in the absence of the event ($\overline{E}$) requiring the ICI operation. The latter is derived by the definition of a spurious operation per se, which means undesirable/unnecessary operation of a function in the absence of the triggering event.

IV. Framework Illustration Using the Cypriot System

This section implements the unified framework (ICI plus risk assessment) on the actual power system of Cyprus.

A. Power System of Cyprus

The Cypriot power system consists of 151 buses, 344 branches and two power stations (i.e., Dhekelia, 460 MW, and Vasilikos, 867.5 MW) with eight and nine synchronous generators, respectively. The complete network parameters, protection settings, as well as the dynamic models and parameters of each generator (i.e., machine, exciter, and governor) have been provided by the TSO and the Electricity Authority of Cyprus [29]. It must be mentioned that loads are modeled as constant power as their dynamic characteristics are currently unavailable. Fig. 7 shows the graph representation of the Cypriot network – fully implemented in DigSilent PowerFactory [30].

B. ICI Scheme in the Cypriot Network

Based on historical demand data, the winter and summer peak demand levels in Cyprus are 848.71 MW and 1187 MW, respectively. They represent the most stressed conditions that the Cypriot system experiences; thus, the analyses below focus on these demand levels (*"worst-case" scenarios*). To demonstrate the effectiveness of the unified framework, feedback from the TSO is used to develop two case studies for each demand level (i.e., two different faults leading to blackout).

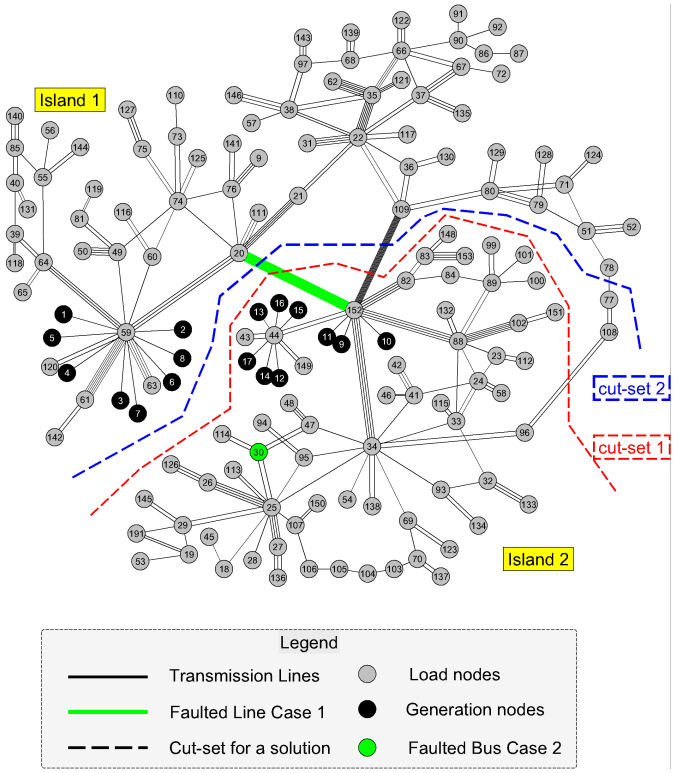

Fig. 7. Graph of the Cypriot network (with optimal islanding solutions)

1) *Case Study 1*

At $t = 1$ s, a three-phase to ground fault occurs near the largest power station (i.e., Vasilikos) at line 20-152 (lines shown in green in Fig. 7). The fault is not cleared by local relays, and instead secondary protection schemes are triggered based on the actual settings of the real system. Indeed, it is important to mention that out-of-step relays disconnect several generators approximately after 1.5 s (see Fig. 8 – Fig. 10). In other words, the system response represents that of the real network given that the TSO has set the protection schemes. The generator rotor angles of the two stations without islanding are shown in Figs. 8 and 9. Shortly after the fault, the generators within each station swing together and those in different ones swing apart. Two groups are created: {1,2,3,4,5,6,7,8} and {9,10,11,12,13,14,15,16,17}.

Although these groups can be created through visualization of the generator rotor angle trends, algorithms to automatically identify coherent groups of generators (e.g., [23], [24]) must be adopted in large-scale systems to ensure adequate generator grouping, and to further improve the unified framework proposed here. In terms of the generators' speed, Fig. 10 shows that they increase. It is noted that such increments cause the tripping of G8 and G7 at 1.798 s and 2.091 s respectively, due to the operation of overspeed protections (set to 1.115 p.u.). Fig. 11 finally highlights that the generator terminal voltages are significantly low. Thus, it can be concluded that the system needs to be split, if the blackout is to be avoided.

Given that this is a very severe disturbance, feedback from the Cyprus TSO has been used to define the necessity to split the system 50 ms after the fault occurs, i.e., at 1.05 s. The ICI method is then implemented considering the power flows and system topology at $t = 1.05$ s. To accelerate the identification of the optimal solution, only twenty free-nodes were included

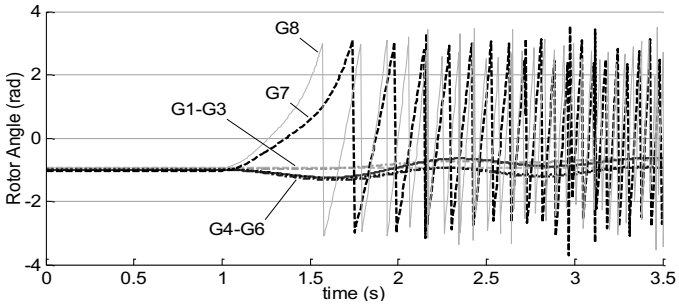

Fig. 8. Generator rotor angles: Power station 1 in Cyprus without islanding

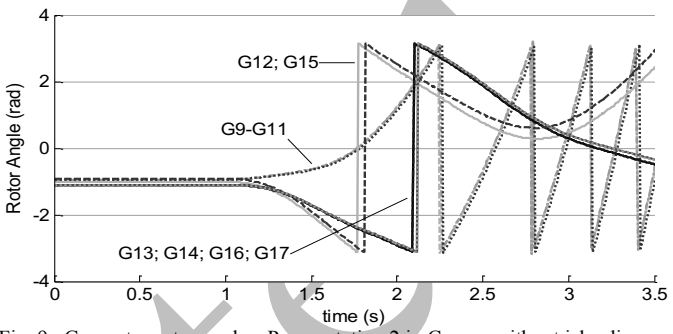

Fig. 9. Generator rotor angles: Power station 2 in Cyprus without islanding

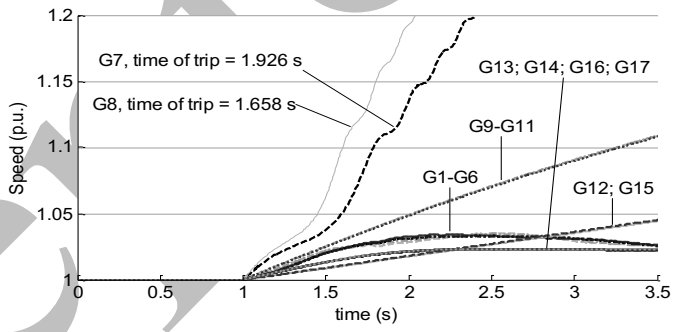

Fig. 10. Generator speeds: Both power stations in Cyprus without islanding

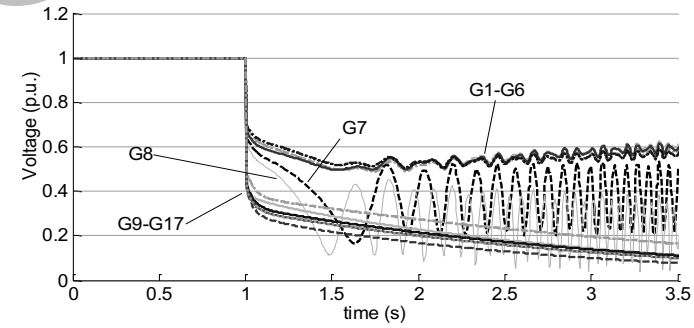

Fig. 11. Generator voltages: Both power stations in Cyprus without islanding

in the combinatorial optimization. The free-nodes were defined considering the electrical distance between groups. Only load buses with similar distance from the coherent groups were included. Generators within each group were labelled accordingly. Transformers and critical lines, defined by the Cyprus TSO, were excluded from the solution space.

The optimal islanding solution is shown in Fig. 7 (cut-set 1, red-dotted line). This solution was found in approximately 0.23 s. Hence, islanding was undertaken at 1.28 s (i.e., t_{imp} = 1.05 s + 0.23 s). It is important to mention that there are a few seconds for islanding after a severe disturbance. In practical implementations, it is expected to have high-performance computers, or even computer clusters, to carry out this critical

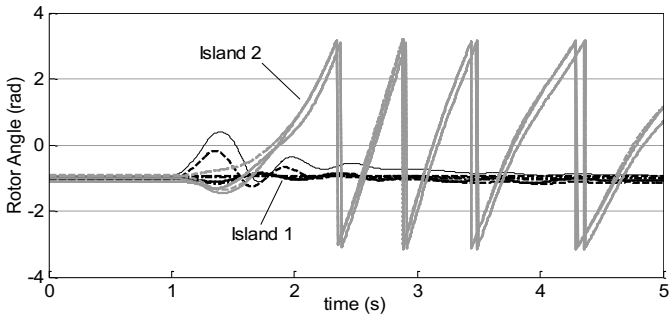

Fig. 12. Generator rotor angles: Both power stations in Cyprus with islanding

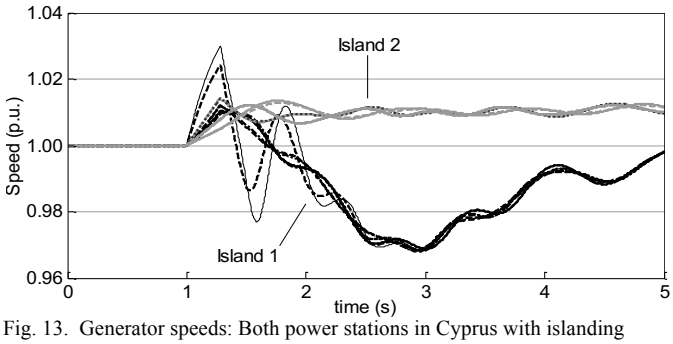

Fig. 13. Generator speeds: Both power stations in Cyprus with islanding

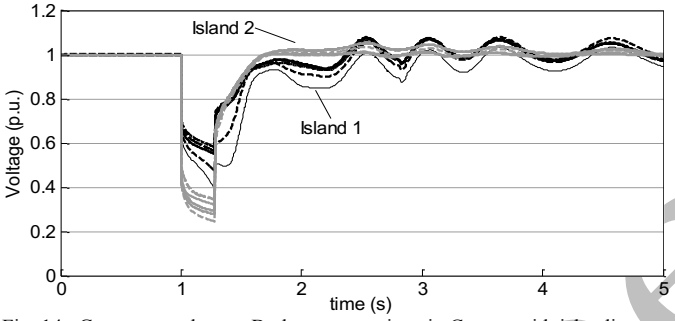

Fig. 14. Generator voltages: Both power stations in Cyprus with islanding

task. For the purpose of this work, it can thus be seen that the proposed ICI method can meet the requirement of real-time controlled islanding in this real system.

The post-islanding behavior of the islands is shown in Figs. 12-14. Fig. 12 shows the generators rotor angle in each island; although the rotor angle trajectories of the generators exhibit an oscillation mode, the two groups of generators oscillate coherently. Moreover, it is expected that in practice the use of additional corrective measures (e.g., fast valving and load shedding) will further be needed in the post-islanding stage to achieve a better dynamic performance.

Fig. 13 further shows that the generator speeds (0.97 p.u. and 1.003 p.u. respectively) are within the limits; defined by the Cypriot TSO as 0.95-1.04 p.u. It is important to mention that 99.57 MW and 208.11 MW of load for the winter and summer peak demand respectively was automatically shed by the protection relays in order to retain the frequency of the created islands within the thresholds. Fig. 14 finally indicates that the generator terminal voltages are successfully kept within the desirable limits (defined as ±10% deviation of the nominal value). This result is important as it highlights that, although voltage constraints are not considered in the proposed ICI method, the solution found using this approach still retains voltages within the statutory thresholds. Consequently, it can be concluded that the proposed ICI method successfully prevents the power system blackout.

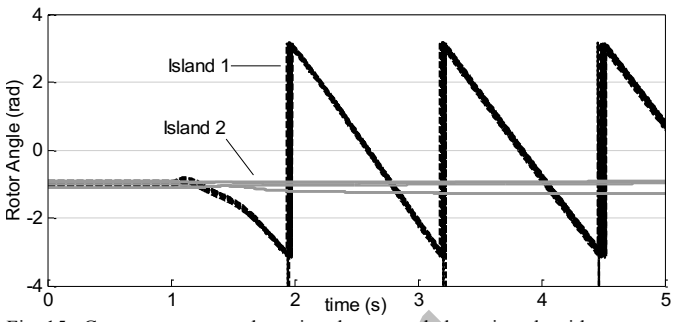

Fig. 15. Generator rotor angles using the spectral clustering algorithm

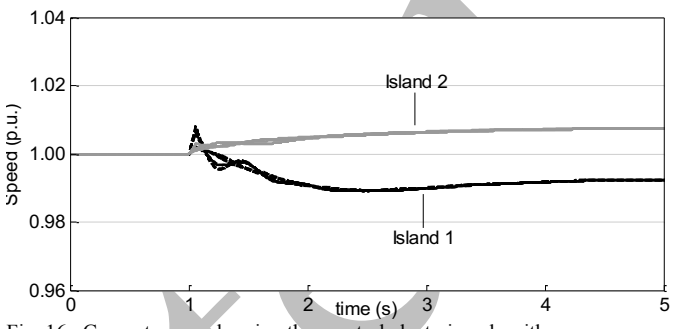

Fig. 16. Generator speeds using the spectral clustering algorithm

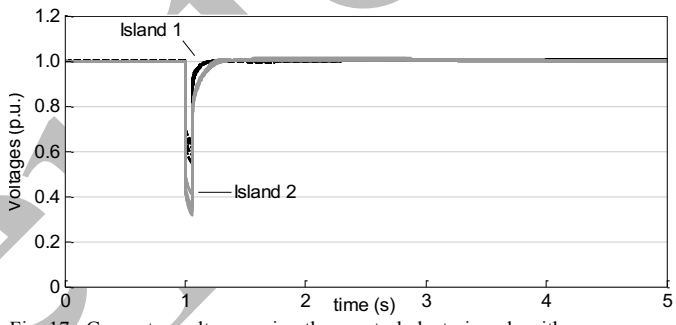

Fig. 17. Generator voltages using the spectral clustering algorithm

2) Case Study 2

At $t = 1$ s, a three phase to ground fault occurs near bus 30 (132 kV substation, node shown in green in Fig. 7), resulting again in the generators within each station to swing together and those in different stations to swing apart. Although not shown here, two groups are created: {1,2,3,4,5,6,7,8} and {9,10,11,12,13,14,15,16,17}. The necessity to split the system is defined to be at 1.5 s. Hence, the ICI method is used to find the optimal islanding solution (considering 20 "free nodes" as well as power flows and topology at t = 1.5 s.). The disturbance analyzed in this case study is not as severe as the one investigated in case study 1. The islanding solution that pro duces the minimal power imbalance is illustrated in Fig. 7 (cut-set 2, blue-dotted line). The optimal islanding solution was found in approximately 0.23 s and islanding was undertaken at 1.73 s. The protection relays did not shed more load into the created islands. Although not shown due to space limitations, the behavior of the system without and with islanding is like the one given in Figs. 8-14 for case study 1.

C. Comparison with Spectral Clustering Algorithm [9]

Case study 1 is now considered to compare the proposed ICI method against an existing one: the spectral clustering algorithm presented in [9]. This algorithm found the solution across lines 20-152, 22-109 and 22-36 in 0.0055 s; hence islanding was undertaken at 1.0555 s. The dynamic response

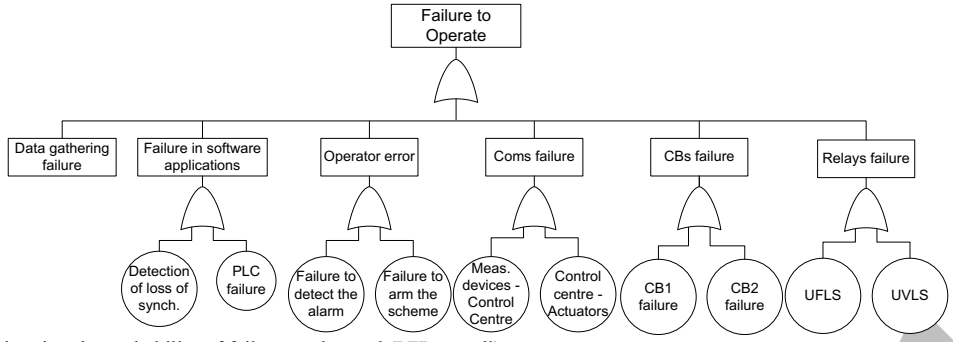

Fig. 18. Fault tree for estimating the probability of failure on demand (PFDoverall)

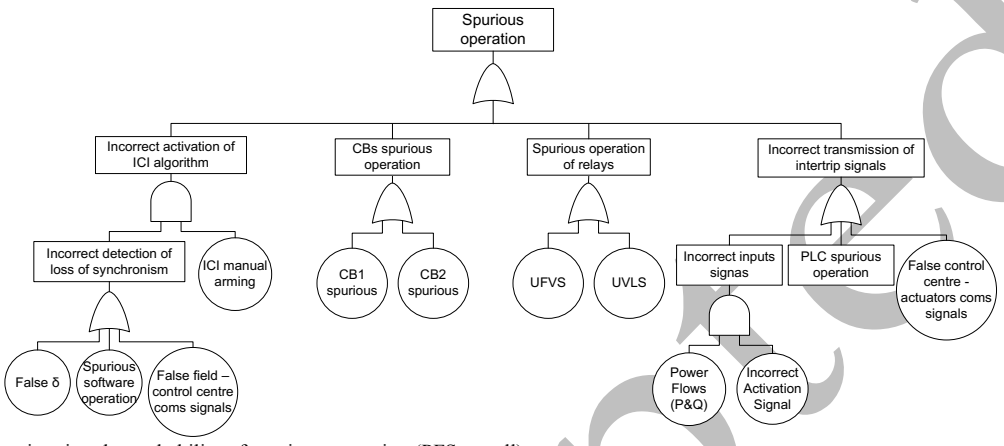

Fig. 19. Fault tree for estimating the probability of spurious operation (PFSoverall)

of the system is shown in Figs. 15-17. Although this solution was found faster than the one with the proposed method, and results in lower power flow disruption, the power imbalance within each island can be as high as 206.247 MW (Island 1), opposite to the 25.056 MW found with the proposed method. In practice, this imbalance results in more load shedding, which, in turn, will have a much higher impact on the system (higher risk on the system as discussed in Section IV-D).

D. Risk Assessment of ICI Method: Cypriot network

Three operational modes of the ICI scheme (and its components) are considered (as done for other SIPS): success, failure to operate and spurious operation. While the impact may vary from one case to another, it is the intention of this paper to produce a framework that will help TSOs in assessing the impact of ICI schemes on their networks. Based on the logic design shown in Fig. 6, Table I presents the main ICI components and their reliability data (extracted from the literature and used for illustrating the risk assessment framework).

The test interval of the components is set to 5 years, based on feedback from the main component manufacturer and provider of the Cypriot network. Due to lack of reliability data, the same MTTF and MTTFS are assumed for each component, which results in equal *PFD* and *PFS*. If a historical database of the electrical utility was available, more accurate MTTF and MTTFS can be used. It can also be seen that the operator is considered as an individual component of the ICI scheme, i.e., operator error. Table I also shows the *PFD* and *PFS* of each ICI component as estimated using (7) and (8), using a simulation period (*TP*) of one year.

1) Fault Trees Design for the Cypriot Network

Figures 18 and 19 present the fault trees for evaluating the $PFD_{overall}$ and $PFS_{overall}$, respectively. They indicate the events and/or combination of events that may lead to a failure of the ICI scheme to operate or to a spurious operation.

Figure 18 indicates that a failure of the ICI scheme to operate as designed can occur due to: (i) a failure in the field data gathering devices; (ii) failure in the software applications for detecting the loss of synchronism or carrying out the logic operation of the scheme (i.e., PLC); (iii) the operator's failure to detect the alarm by the information/alarm processing system or failure to manually arm in service the ICI method in a timely manner; (iv) a communication failure between field – control center and vice-versa; (v) a failure in the CBs to open the lines determined by the ICI solution, which will consequently result in the failure of the scheme to split the network into stable islands; and/or vi) a failure in the underfrequency or undervoltage load shedding relays (UFLS and UVLS respectively) to shed load for balancing the formed islands. In this work, and like the risk assessments available in the literature, it is considered that the failure to operate as designed of one single ICI component leads to the complete failure of the overall ICI scheme – this may vary among TSOs.

Figure 19 further shows that a spurious operation of the ICI scheme may occur due to: (i) an incorrect activation of the ICI solution which will occur in case of an incorrect detection of loss of synchronism and manual arming by the operator; (ii) an incorrect transmission of intertrip signals; (iii) a spurious operation of CBs, and/or iv) a spurious operation of the UFLS and UVLS relays, i.e., shed load when not required. As above, and like other risk assessments, it is considered that the spurious operation of one single ICI component leads to the complete spurious operation of the overall ICI scheme – and again this may vary among TSOs.

TABLE I
RELIABILITY DATA OF ICI COMPONENTS

ICI Component	MTTF/MTTFS (years)	PFD ($x10^{-3}$)	PFS ($x10^{-3}$)
Data gathering	400	6.25	2.5
Detection of Loss of Synchronism	300	8.33	3.33
UFLS relays	500	5	2
UVLS relays	500	5	2
Communication links	500	5	2
Circuit breakers	1700	1.47	0.58
PLC	300	8.33	3.33
Operator error	1000	2.5	1

The fault trees shown in Figs. 18 and 19 are generic (as the logic in Fig. 6) and can be applied to any ICI scheme. Indeed, if the detailed architecture of the ICI scheme becomes available, then these fault trees can be extended to cater for any other IC component. The events considered were selected as they have been taken into account in past reliability studies of other SIPS [14], [28]. Finally, the fault trees were designed based on feedback from the Cypriot TSO, and can be easily adapted if further needs are required.

2) Risk Assessment in the Cypriot Network

The *PFD* and *PFS* of the individual component of Table I are now inserted in the fault trees of Figs. 18 and 19 for quantifying $PFD_{overall}$ and $PFS_{overall}$. The risk assessment is carried out only for the two case studies discussed above, as they are of interest in this work. Tables II and III show the probabilities of the ICI operational modes, the load shedding occurring due to each ICI operational mode, and the overall risk without and with the ICI in operation for the two case studies and demand levels (i.e., winter and summer peak demands). The VoLL for the Cypriot system is considered equal to 6,500 €/MWh, based on a typical value reported in [31], and the probability of the electrical event per year, *P(E)*, equal to $1x10^{-2}$, based on feedback from the TSO.

To define the risk without ICI in operation, the case studies presented in Section IV-B that resulted in the complete blackout of the Cypriot system are considered. The impact *Im(E)* (i.e., using the load shedding) for the winter and summer peak demands is equal to 848.71 MW and 1187 MW, respectively. Thus, the risk without ICI can be calculated using (9)-(10).

The risk with ICI in operation is estimated using (11)-(14). Note that the impact of an ICI failure to operate is equal to the impact without the ICI in operation. The risk assessment results are shown in Tables II and III for case studies 1 and 2, respectively. In these tables, the probabilities of the ICI operational modes and the resulting load shedding and risk per hour of the interruption duration are given.

3) Analysis of the Risk in the Cypriot Network

For case study 1 (Table II), in the winter peak demand study and for a successful ICI operation, the risk is reduced from 55.16 to 6.17 ($\times 10^3$ €/h). This difference is also high for the summer peak demand, i.e., from 77.15 to 12.89 ($\times 10^3$ €/h). Despite the analyzed peak demand, a successful operation of the ICI scheme in case study 2 (Table III) leads to no load shedding, i.e., no risk is introduced by the successful operation of the ICI scheme. Finally, it must be noted that a high risk is introduced by a spurious operation during summer, i.e., 17.62 and 16.87 ($\times 10^3$ €/h) for the two case studies. An incorrect scheme operation during highly stressed conditions results in a high amount of load shedding for creating two stable islands.

TABLE II
RISK ASSESSMENT RESULTS FOR CASE STUDY 1

	Probability of Event/ICI Operation		Load shedding (MW)		Risk ($x10^3$ €/h)	
			Winter	Summer	Winter	Summer
W/o ICI	$P(E)$	0.01	848.71	1187	55.16	77.15
With ICI	$P(E)\times(1-PFD_{overall})$	9.53×10^{-3}	99.57	208.11	6.17	12.89
	$P(E)\times PFD_{overall}$	4.7×10^{-4}	848.71	1187	2.59	3.62
	$P(\bar{E})\times PFS_{overall}$	1.05×10^{-2}	42.78	260.8	2.89	17.62
	Total Risk with ICI ($x10^3$ €/h)				11.65	34.13
	Risk decrease (%)				78.88	55.76

TABLE III
RISK ASSESSMENT RESULTS FOR CASE STUDY 2

	Probability of Event/ICI Operation		Load shedding (MW)		Risk ($x10^3$ €/h)	
			Winter	Summer	Winter	Summer
W/o ICI	$P(E)$	0.01	848.71	1187	55.16	77.15
With ICI	$P(E)\times(1-PFD_{overall})$	9.53×10^{-3}	0.00	0.00	0	0
	$P(E)\times PFD_{overall}$	4.7×10^{-4}	848.71	1187	2.59	3.62
	$P(\bar{E})\times PFS_{overall}$	1.05×10^{-2}	39.79	249.66	2.69	16.87
	Total Risk with ICI ($x10^3$ €/h)				5.28	20.49
	Risk decrease (%)				90.43	73.44

Comparing the total risk without and with ICI, a significant decrease in the risk is observed for both case studies, with the risk decrease being significantly higher for the winter peak demand than for the summer peak demand. This shows the effectiveness of the proposed ICI algorithm and its contribution as an emergency control action to mitigating the risk of the disturbance, even during peak demand conditions. These results also show that even when the uncertainty associated with its reliability is considered, the risk with the ICI in operation is significantly lower. This is due to the fact that the probability of an ICI undesirable operation is low and, additionally, the amount of load shedding required for stabilizing the islands is much lower than the load shedding following a complete blackout, as shown in Tables II and III. This altogether leads to a much lower risk with the ICI scheme in operation.

E. Effects of Adding Redundancy to the ICI Scheme

The effects of adding full redundancy to the ICI scheme on the risk evaluation are now evaluated, which affects the reliability analysis as follows (details can be found in [17]):

- A failure of both the primary and secondary (redundant) component needs to occur for a function to fail to be executed when required (i.e., $PFD_{overall}$ is decreased).
- A spurious operation of either the primary or the secondary component is capable of incorrectly activating a function and triggering the scheme (i.e., $PFS_{overall}$ increases).

Therefore, on the one hand, an improvement in the risk by a failure of the ICI scheme to operate can be observed; however, on the other hand, adding redundancy results in an increase in the risk introduced by a spurious operation of the ICI scheme.

Table IV summarizes the results of this analysis. By adding full redundancy, the risk decrease with the ICI in operation for the winter peak demand study remains approximately the same for case studies 1 and 2, i.e., 77.67 and 90.12% respectively (compared to 78.88 and 90.43% without redundancy). This means that the improvement in the risk by reducing

TABLE IV
RISK DECREASE BY ADDING FULL REDUNDANCY TO THE ICI SCHEME

Case Study	Risk Decrease (%)	
	Winter	Summer
1	77.67	36.68
2	90.12	56.14

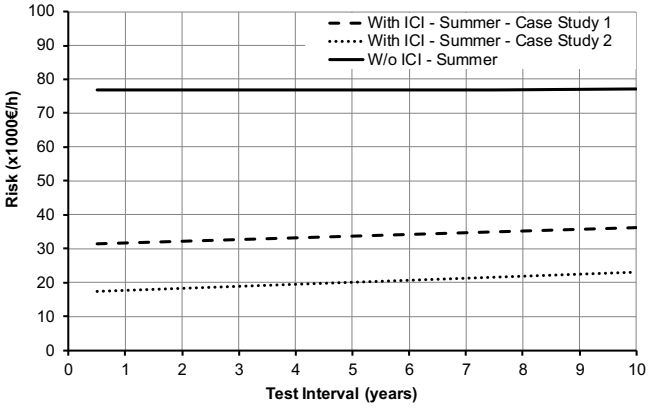

Fig. 20. Effect of ICI scheme's test interval (TI) on overall system risk for the summer peak demand

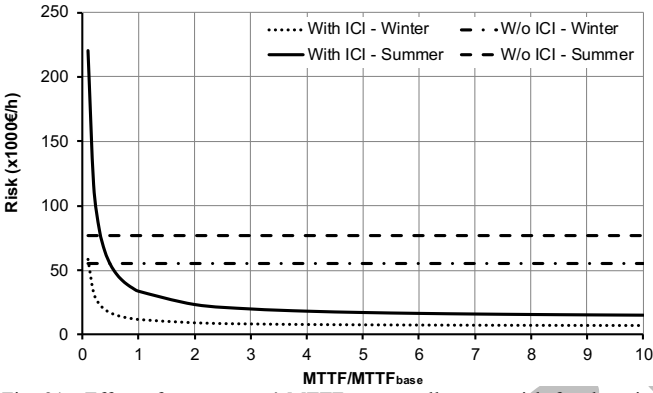

Fig. 21. Effect of components' MTTF on overall system risk for the winter and summer peak demand, case study 1

$PFD_{overall}$ compensates for the increase in the risk due to a higher $PFS_{overall}$. On the other hand, for the summer peak demand study, the risk decrease reduces to 36.68 and 56.14% for the case studies 1 and 2 from 55.76 and 73.44% respectively.

This is because a higher load shedding occurs for the summer peak demand from a spurious operation of the ICI scheme, i.e., 260.8 and 249.66 MW for case studies 1 and 2 respectively (compared to 42.78 and 39.79 MW respectively for the winter peak demand), which in combination with the increase in $PFS_{overall}$ due to the full redundancy added to the scheme, results in high risk by a spurious operation.

F. Sensitivity Analysis

In order to tackle the uncertainty associated with the reliability data used, sensitivity studies are performed in this section. In particular, based on (7)-(8) the test interval and the MTTF of the components are varied to evaluate their impact on the estimated risk with the ICI in operation.

1) Varying components' test interval (TI)

The test interval of the ICI scheme has been varied in the range of [0.5, 10] years with a step of 0.5 years. Fig. 20 shows the results of this analysis only for the summer peak demand studies (it has a higher risk than the winter peak demand, see Tables II and III). The increase in the *TI* results in an increase in the risk introduced by the ICI. However, the slope of the risk curves with ICI in operation is smooth, and as a result they do not cross the risk curve without (w/o) ICI, even for the highest *TI* used here, i.e., 10 years. It is not expected that such a scheme of vital importance for the stability of a network will not be tested and maintained with a frequency lower than 10 years (this may vary among TSOs). It can therefore be concluded that the *TI* is not a determining factor that can result in higher risks by having the proposed ICI scheme in operation.

2) Varying components' MTTF

The ICI components' MTTF (and MTTFS) has been varied in the range of [0.1x$MTTF_{base}$, 10x$MTTF_{base}$], where $MTTF_{base}$ refers to the components' MTTF and MTTFS presented in Table I. Fig. 21 shows the results of this analysis for case study 1, for the winter and summer peak demands. Similar results are obtained for case study 2.

As can be seen in Fig. 21, the risk w/o ICI in operation becomes lower than the risk with ICI for much lower values of MTTF compared to the ones of Table I (approximately 0.1×$MTTF_{base}$ and 0.3×$MTTF_{base}$ for the winter and summer peak demand case studies respectively). In fact, based on experience and on published reliability data of the components of Table I, it is quite easy and possible to achieve higher MTTF than these values; hence it is rather impossible to obtain higher risks with the proposed ICI in operation using the available components by the manufacturers for realizing the scheme. It can also be observed that as the MTTF of the ICI components increases, the decline in the risk becomes smoother, which will ultimately converge to values close to the risk by a successful ICI operation (but not equal, because even though the risk of failure and spurious operations will be very low, it will still be higher than zero).

V. CONCLUSIONS

This paper has presented a unified framework that first introduces an effective ICI scheme and then assesses the risk of the system with the ICI scheme in operation to tackle the uncertainty and concerns related to the reliability of such schemes. Considering the increasing complexity and vulnerability of power systems to electrical disturbances, such a systematic and comprehensive analysis becomes critical and contributes significantly to the decision-making on the most appropriate reliability enhancement and investment strategies.

The proposed ICI scheme is based on the well-established cut-set matrix concept, which is modeled as a combinatorial optimization problem with constraints. The objective function of this problem is the minimum power imbalance within islands, while the main constraints are the coherent generator groups and transmission line availability. The proposed ICI algorithm is tested using the IEEE 9-bus system and the real Cypriot system. Different case studies (i.e., faults) and demand levels are examined for illustrating the ICI algorithm using the Cypriot network, which demonstrates its adaptability and effectiveness in minimizing the impact of cascading outages leading to blackouts under varying system conditions.

Further, the application of the fault tree-based risk assessment methodology using the ICI scheme applied on the Cypriot network shows that the overall system risk is significantly

reduced when the ICI scheme is in operation. This indicates that the system robustness to sudden electrical contingencies is enhanced with the proposed ICI scheme, even when the probability of the scheme's failure modes is considered.

Simulation results of adding redundancy and considering sensitivity analysis are carried out to provide useful insights on the aspects affecting the reliability of the proposed ICI scheme, and thus the risk introduced by their undesirable operations. The unified framework presented in this paper can provide an effective solution in mitigating the effect of large disturbances, as well as estimating the risk associated with an undesirable operation of the ICI scheme. If the relevant data are available, then the unified framework proposed here can be applied to any power system, which would provide insights on the benefits and risks of applying the ICI scheme.

REFERENCES

[1] G. Andersson *et al.*, "Causes of the 2003 major grid blackouts in North America Europe, and recommended means to improve system dynamic performance," *IEEE Trans. Power Syst.*, vol. 20, no. 4, pp. 1922–1928, Nov. 2005.

[2] P. Kundur and C. W. Taylor, "Blackout experiences and lessons, best practices for system dynamic performance, and the role of new technologies," final report, May 2007.

[3] M. M. Adibi, R. J. Kafka, S. Maram, and L. M. Mili, "On power system controlled separation," *IEEE Trans. Power Syst.*, vol. 21, no. 4, pp. 1894–1902, Nov. 2006.

[4] H. You, V. Vittal, and X. Wang, "Slow coherency - Based islanding," *IEEE Trans. Power Syst.*, vol. 19, no. 1, pp. 483–491, Feb. 2004.

[5] G. Xu and V. Vittal, "Slow coherency based cutset determination algorithm for large power systems," *IEEE Trans. Power Syst.*, vol. 25, no. 2, pp. 877–884, May 2010.

[6] G. Xu, V. Vittal, A. Meklin, and J. E. Thalman, "Controlled Islanding Demonstrations on the WECC System," *IEEE Trans. Power Syst.*, vol. 26, no. 1, pp. 334–343, Feb. 2011.

[7] A. Peiravi and R. Ildarabadi, "A fast algorithm for intentional islanding of power systems using the multilevel kernel k-means approach," *J. Appl. Sci.*, vol. 9, no. 12, pp. 2247–2255, Jan. 2009.

[8] R. Sánchez-García *et al.*, "Hierarchical clustering of power grids," *IEEE Trans. Power Syst.*, vol. 29, no. 5, pp. 2229–2237, Sept. 2014.

[9] J. Quiros-Tortos *et al.*, "Constrained Spectral Clustering Based Methodology for Intentional Controlled Islanding of Large-Scale Power Systems," *IET Gener. Transm. Distrib.*, vol. 9, no. 1, pp. 31–42, Jan. 2015.

[10] K. Sun, D. Z. Zheng, and Q. Lu, "Splitting strategies for islanding operation of large-scale power systems using OBDD-based methods," *IEEE Trans. Power Syst.*, vol. 18, no. 2, pp. 912–923, May 2003.

[11] C. Wang, B. Zhang, Z. Hao, J. Shu, P. Li, and Z. Bo, "A novel real-time searching method for power system splitting boundary," *IEEE Trans. Power Syst.*, vol. 25, no. 4, pp. 1902–1909, Nov. 2010.

[12] K. Sun, K. Hur, and P. Zhang, "A New Unified Scheme for Controlled Power System Separation Using Synchronized Phasor Measurements," *IEEE Trans. Power Syst.*, vol. 26, no. 3, pp. 1544–1554, Aug. 2011.

[13] R. Franco, C. Sena, G. N. Taranto, and A. Giusto, "Using synchrophasors for controlled islanding—A prospective application for the Uruguayan power system," *IEEE Trans. Power Syst.*, vol. 28, no. 2, pp. 2016–2024, May 2013.

[14] W. Fu, S. Zhao, J. D. McCalley, V. Vittal, and N. Abi-Samra, "Risk Assessment for Special Protection Schemes," *IEEE Trans. Power Syst.*, vol. 17, no. 1, pp. 63–72, Feb. 2002.

[15] M. Esmaili, A. A. Hajnoroozi, and H. A. Shayanfar, "Risk evaluation of online special protection systems," *Int. J. Electr. Power Energy Syst.*, vol. 41, no. 1, pp. 137–144, Oct. 2012.

[16] PSERC, "System Protection Schemes: Limitations, Risks, and Management," Final project report, Dec. 2010.

[17] M. Panteli, P. Crossley, and J. Fitch, "Quantifying the reliability level of system integrity protection schemes," *IET Gener. Transm. Distrib.*, vol. 8, no. 4, pp. 753–764, Apr. 2014.

[18] ESB and National Grid, "Report on investigation into System Disturbance of August 5th 2005," Dec. 2005.

[19] J. Quirós-Tortós, M. Panteli, P. Wall, and V. Terzija, "Sectionalising methodology for parallel system restoration based on graph theory," *IET Gener. Transm. Distrib.*, vol. 9, no. 11, pp. 1216–1225, Aug. 2015.

[20] W. K. Chen, *Graph theory and its engineering applications*, Advanced Series in Electrical and Computer Engineering: vol. 5, Singapore: World Scientific Publishing, 1997.

[21] P. Pourbeik, P. Kundur, and C. W. Taylor, "The anatomy of a power grid blackout - Root causes and dynamics of recent major blackouts," *IEEE Power and Energy Mag.*, vol. 4, no. 5, pp. 22–29, Sept.-Oct. 2006.

[22] M. Panteli, P. Crossley, D. S. Kirschen, and D. J. Sobajic, "Assessing the Impact of Insufficient Situation Awareness on Power System Operation," *IEEE Trans. Power Syst.*, vol. 28, no. 3, pp. 2967–2977, Aug. 2013.

[23] S. B. Yusof, G. J. Rogers, and R. T. H. Alden, "Slow coherency based network partitioning including load buses," *IEEE Trans. Power Syst.*, vol. 8, no. 3, pp. 1375–1382, Aug. 1993.

[24] M. Jonsson, M. Begovic, and J. Daalder, "A new method suitable for real-time generator coherency determination," *IEEE Trans. Power Syst.*, vol. 19, no. 3, pp. 1473–1482, Aug. 2004.

[25] C. Moler, *Numerical Computing with MATLAB*. Society for Industrial and Applied Mathematics, 2004.

[26] P. Demetriou, M. Asprou, J. Quiros-Tortos, and E. Kyriakides, "Dynamic IEEE Test Systems for Transient Analysis," *IEEE Syst. Journal*, vol. PP, no. 99, pp. 1–10, Jun. 2015.

[27] U.S. Nuclear Regulatory Commission, "Fault Tree Handbook," NUREG-0492, Jan. 1981.

[28] Tsun-Yu Hsiao and Chan-Nan Lu, "Risk Informed Design Refinement of a Power System Protection Scheme," *IEEE Trans. Reliab.*, vol. 57, no. 2, pp. 311–321, Jun. 2008.

[29] "Electricity Authority of Cyprus." [Online]. Available: https://www.eac.com.cy/EN/CustomerService/Pages/default.aspx.

[30] "DIgSILENT PowerFactory - Power System Analysis and Engineering." [Online]. Available: http://www.digsilent.de/.

[31] T. Zachariadis and A. Poullikkas, "The costs of power outages: A case study from Cyprus," *Energy Policy*, vol. 51, pp. 630–641, Dec. 2012.